Cooperative Structure Directing Role of the Cage-Forming Tetramethylammonium Cation and the Bulkier Benzylmethylpyrrolidinium in the Synthesis of Zeolite Ferrierite

Ana Belen Pinar, Luis Gomez-Hortiguela, and Joaquin Perez-Pariente*

Instituto de Catalisis y Petroleoquimica (CSIC), c/Marie Curie 2, Cantoblanco, 28049-Madrid, Spain

Received July 3, 2007. Revised Manuscript Received September 3, 2007

Hydrothermal synthesis of zeolites often requires the presence of an organic molecule or structure directing agent (SDA), which participates in the organization of the inorganic tetrahedral units into a particular topology. Bulky molecules are frequently employed as SDAs in attempts to obtain large-pore zeolite structures. However, many open-framework zeolitic structures are composed of small cages apart from the wide channels, and only small SDAs can be accommodated within these cages. These observations leaded us to design a synthesis strategy based on the combination of small molecules with bulkier cations as SDAs. The simultaneous use of tetramethylammonium (TMA) and the bulkier benzylmethylpyrrolidinium (bmp) as SDAs has led to the crystallization of the zeolite ferrierite from gels having a Si/Al ratio in the range of 16−10, in fluoride medium and in the absence of inorganic cations. Molecular mechanics calculations revealed the templating role of both cations, as the most stable configuration of the system corresponds to the siting of TMA within the FER cages, while bmp accommodates in the 10 membered-ring one-dimensional channels. Ferrierite is not obtained in the absence of either TMA or bmp, thus evidencing the co-structure directing role in the crystallization process of this zeolite.

Introduction

Zeolites, a class of microporous crystalline aluminosilicate materials, have been extensively studied over the last 50 years.[1] The three-dimensional networks of these microporous materials are composed of corner-sharing tetrahedral SiO_4 and AlO_4 units linked through oxygen atoms. The hydrothermal synthesis, particularly for high silica zeolites, usually requires the addition of organic molecules to the synthesis gel, which act as structure directing agents (SDAs) during the crystallization of microporous frameworks. Since the pioneering work of Barrer and Denny,[2] the use of water-soluble organic molecules, especially amines and quaternary ammonium cations, has allowed the discovery of a large number of new zeolite topologies, as well as making accessible different compositions of those materials. The concept of templating has been described[3] as the phenomenon occurring during either the gelation or the nucleation processes, whereby the organic molecule organizes the oxide tetrahedral units into a particular geometric topology around itself and thus provides the initial building blocks for the crystallization of a particular structure type. Hence, the organic molecules are encapsulated during the crystallization of the microporous framework and thus contribute to the final stability of the system through the development of nonbonded interactions between them.

Many studies show that in most cases, the SDA should fit itself to the nascent structure, if this is finally to survive during the nucleation period. Bulky templates are preferentially used in an attempt to obtain large-pore structures; however, this probably imposes the necessity of assembling a relatively large number of TO_4 units around the SDA during the nucleation step, which explains the long induction period often observed. In these conditions, the crystallization process may not be energetically favorable, leading to the formation of amorphous materials or, eventually and very often, to mixtures of phases. In this context, the presence of small organic species in the synthesis gel could assist the crystallization process by preorganizing the TO_4 units around them, giving place to building units that could be more easily assembled by the bulkier organic SDAs, thus helping to overcome the nucleation energy barrier. The arrangement of tetrahedral TO_4 units around a less bulky SDA to form organized inorganic entities would not require such a large increase in the structural ordering of the system. The building-up process of crystalline structures would hence be favored by creating a "soup" rich in organic compounds, which could contain eventually inorganic cations as well. In these conditions, a variety of SDA molecules, and therefore a variety of organo−inorganic building units, would be offered to the system, and the most energetically stable zeolite among the possible structures that could be built-up in the presence of these templates would crystallize. The underlying strategy is basically to increase the viable condensation pathways of the silica or aluminosilicate oligomers present in the synthesis medium.

Close examination of the most open zeolite frameworks reveals that structures composed of a combination of small

* Corresponding author. Tel.: +34 91 5854784; fax: +34 91 5854760; e-mail: jperez@icp.csic.es.

(1) Breck, D. W. *Zeolite Molecular Sieves*; John Wiley and Sons: New York, 1974.
(2) Barrer, R. M.; Denny, P. J. *J. Chem. Soc.* **1961**, 971.
(3) Lok, B. M.; Cannan, T. R.; Messina, C. A. *Zeolites* **1983**, *3*, 282.

10.1021/cm071753o CCC: $37.00
Published on Web 10/23/2007

cages and larger cavities and/or channels predominate, such as FAU, LTA, CHA, or PAU topologies or the more recent SSZ-35,[4] to name a few. However, only small SDA molecules can be accommodated within the small cages, while the usual bulky SDA molecules preferred for the synthesis of large-pore materials cannot fit in such small cages. All these observations led us to believe that a variety of microporous structures could be obtained from all-silica or Al-poor synthesis gels by combining bulky SDA and small molecules or even inorganic cations as well. It is worth mentioning here that some clathrate hydrates, containing cages of different sizes, also require a combination of small and large molecules to form,[5] and in the field of zeolite synthesis, the structure directing role of fluoride anions entrapped in small cages has been discussed.[41]

Therefore, we rationally followed a synthesis strategy based on the use of a combination of small molecules with bulkier SDAs with the aim that each one of them plays a specific role in the building-up process of crystal structures: the small cation would promote the formation of cages, while the bulkier one would assemble these cavities to form the structure finally obtained.

In the present work, we have aimed at exploring the co-structure directing role of the tetramethylammonium cation (TMA) and the bulkier benzylmethylpyrrolidinium cation (bmp). It is well-known that the TMA cation favors the formation of cavities. In fact, since its first use in the 1960s,[2,6] more than 17 different structures have been made with TMA, and most of them contain cavities. Some examples of these zeolites are ZK-4 (LTA),[7] having sodalite cages, and omega (MAZ),[8] E (EAB), and offretite (OFF),[9] which contain gmelinite cages. In some cases, TMA has been unambiguously located in the cavities of the zeolite frameworks by ^{13}C CP/MAS NMR, as in ZK-4,[10] offretite,[11] and SAPO-37.[12] Therefore, we chose this cation to act as the small cation in our synthesis strategy. The bmp cation has been thought to be a suitable cation to play the role of the bulky cation. On the one hand, in principle, it can be thought that bmp will not fit within common zeolitic cages, thus avoiding the competition with TMA to be accommodated in these cavities. On the other hand, due to its size, the bmp cation could direct the formation of at least medium-pore size zeolites, which are interesting materials for many catalytic applications. We were interested in investigating the role that each organic molecule plays during the building-up process of the zeolite structure and how it determines the nature of the crystalline product finally obtained. With this aim, we have performed syntheses employing a mixture of TMA and bmp cations as SDAs, varying the amount of TMA in the gel, as well as syntheses in the presence of only one of these two cations. A subsequent computational study based on molecular mechanics was carried out in an attempt to clarify the role of the organic cations in directing the crystallization of the microporous structures, studying the location and interaction energies of the molecules within the framework.

Experimental Procedures

All the experiments were carried out in fluoride medium at low water content since, in this medium, the crystallization of low framework density phases is favored at a low H_2O/SiO_2 ratio.[13]

The synthesis of benzylpyrrolidine was carried out by carefully adding benzyl chloride (50% molar excess) (Sigma-Aldrich, 99 wt %) drop by drop to a solution of pyrrolidine (Sigma-Aldrich, 99 wt %) in ethanol in the presence of potassium carbonate, heating the reaction mixture at 90 °C for 48 h. After completion of the reaction (monitored by the release of CO_2), the reaction mixture containing the tertiary amine was filtered to remove the inorganic solid residues, and the solid residue was washed with ethanol. The solvent was then removed under vacuum at 60 °C, and benzylpyrrolidine was purified by vacuum distillation (110 °C at a pressure of 17 mmHg). The purity of the tertiary amine was assessed by thin layer chromatography (hexane/ethyl acetate as the solvent) and chemical analysis (calculated values, in wt %: C, 82.0; N, 8.7; H, 9.3; found: C, 81.5; N, 8.7; H, 9.9).

The bmp cation, as its iodide salt, was obtained by methylation of benzylpyrrolidine with methyl iodide (50% molar excess, Fluka) in ethanol. The reaction mixture was kept in an ice bath for the first 30 min and stirred for 5 days at room temperature. Ethanol was then removed under vacuum at 60 °C, and the resulting bmp iodide solid was exhaustively washed with diethyl ether until the resulting liquid was colorless. The molecular structure of the collected yellow solid was determined by chemical analysis (calculated values, in wt %: C, 47.5; N, 4.6; H, 5.9; found: C, 47.3; N, 4.7; H, 5.8) and ^{13}C CP/MAS NMR (Figure 6), confirming the identity of the bmp cation (bmp). The iodide salt was then converted into the corresponding hydroxide salt (bmpOH) by ion exchange through an Amberlyst IRN78 resin (exchange capacity: 4 mequiv/g, Supelco). The obtained solution of bmpOH was filtered to remove the resin and titrated with 0.05 M HCl (Panreac) using phenolphthalein (Aldrich) as an indicator.

Zeolite products were obtained from synthesis gels in which the total concentration of organic compounds was kept constant. The molar gel composition for the samples with bmp and TMA as SDAs was 0.969 SiO_2/0.031 Al_2O_3/x TMAOH/(0.54 − x) bmpOH/0.48 HF/4.65 H_2O, where x was 0.06 (bmp-TMA-1 gel) or 0.012 (bmp-TMA-2 gel). For the tetrabutylammonium (TBA)−TMA gel, synthesized with TBA and TMA as SDAs, the gel composition was the same as in bmp-TMA-1 but with TBA instead of bmp. In the syntheses with only one SDA, to maintain the total concentration of organic compounds, the same molar composition was used but with 0.54 bmp (bmp gel) or 0.54 TMA (TMA gel).

The gels were prepared by adding tetraethylorthosilicate (TEOS, Merck, 98 wt %) and aluminum isopropoxide (Fluka, 97 wt %) to an aqueous solution containing the SDAs (bmpOH and TMAOH). The solution was stirred until all the ethanol coming up from the hydrolysis of TEOS and the excess of water evaporated. Subsequently, HF (Panreac, 48 wt %) was added dropwise. The resulting

(4) Wagner, P.; Nakagawa, Y.; Lee, G. S.; Davis, M. E.; Elomari, S.; Medrud, R. C.; Zones, S. I. *J. Am. Chem. Soc.* **2000**, *122*, 263.
(5) Koh, C. A. *Chem. Soc. Rev.* **2002**, *31*, 157
(6) Barrer, R. M.; Denny, P. J.; Flanigen, E. M. Molecular sieves adsorbents. U.S. Patent 3,306,922, 1967.
(7) Kerr, G. T. *Inorg. Chem.* **1966**, *5*, 1537.
(8) Aiello, R.; Barrer, R. M. *J. Chem. Soc. A* **1970**, 1470.
(9) Whyte, T. E., Jr.; Wu, L. E.; Kerr, G. T.; Venuto, P. B. *J. Catal.* **1971**, *20*, 88.
(10) Jarman, R. H.; Melchior, M. T. *J. Chem. Soc., Chem. Commun.* **1984**, *7*, 414.
(11) Hayashi, S.; Suzuki, K.; Shin, S.; Hayamizu, K.; Yamamoto, O. *Chem. Phys. Lett.* **1985**, *113*, 368.
(12) Kovalakova, K.; Wouters, B. H.; Grobet, P. J. *Microporous Mesoporous Mater.* **1998**, *22*, 193.
(13) Camblor, M. A.; Villaescusa, L. A.; Díaz-Cabañas, M. J. *Top. Catal.* **1999**, *9*, 59.

thick gel was manually homogenized (pH ca. 10) and introduced into 20 mL Teflon-lined stainless steel autoclaves that were heated statically at 150 °C and autogenous pressure for selected periods of time. The solid products were recovered by filtration; washed first with water, then with ethanol, and finally with water again; and dried at room temperature overnight.

Solid products were characterized by XRD (PANalytical X'Pert PRO-MPD diffractometer, Cu Kα radiation), FTIR spectroscopy using the KBr pellet technique (Nicolet 5ZDX FTIR spectrometer provided with an MCT detector), thermal analysis (PerkinElmer TGA7 instrument, heating rate 20 °C/min, air flow 30 mL/min, temperature range 20−900 °C), chemical CHN analysis (PerkinElmer 2400 CHN analyzer), ICP-AES (Optima 3300 DV PerkinElmer), SEM/EDX (Jeol JSM 6400 Philips XL30, operated at 20 kV), and solid-state nuclear magnetic resonance. MAS NMR spectra were recorded with a Bruker AV 400 spectrometer using a BL7 probe for ^{13}C, a BL4 probe for ^{27}Al, and a BL2.5 probe for ^{19}F. ^{13}C CP spectra were recorded using $\pi/2$ rad pulses of 4.5 μs and a recycle delay of 3 s. For the acquisition of the ^{13}C spectra, the samples were spun about the magic angle at a rate of 5−5.5 kHz. The ^{27}Al spectra were measured using pulses of 1 μs to flip the magnetization $\pi/12$ rad and delays of 1 s between two consecutive pulses. The ^{27}Al spectra were recorded while spinning the samples at ca. 11 kHz. For ^{19}F, $\pi/2$ rad pulses of 4.5 μs recycle delays of 80 s and spinning rates of approximately 20 kHz were used.

Computational Details. The geometry of the FER structure has been kept fixed during all the calculations. Molecular structures and interaction energies of the SDAs (TMA and bmp) with the framework were described with the CVFF forcefield,[14] in which the van der Waals and electrostatic interactions were explicitly included. These terms were calculated by use of the Ewald summation, excluding the bonded (1−2 and 1−3) interactions. Periodic boundary conditions (PBC) were applied to ensure effective treatment of SDA−SDA interactions.

TMA molecules were first inserted in the FER structure using a Grand Canonical (pVT ensemble) Monte Carlo (MC) procedure,[15] where Coulomb interactions were explicitly included. In these calculations, the coordinates of both the FER structure and the TMA molecules were kept fixed. A total of 2.5 million configurations was sampled, with a constant TMA partial pressure of 100 or 1000 kPa, and a 1 × 1 × 1 unit cell FER system. Framework charges were kept fixed to 2.4 and −1.2 for silicon and oxygen, respectively. The atomic charges for TMA were calculated by the charge-equilibration method,[16] setting the total net charge to +1 and then averaging it to 0 to obtain a neutral sorbate.

The interaction energies of the TMA molecules with the FER structure (one TMA molecule in a 1 × 1 × 1 unit cell FER system) in the two different locations (within the cavity or in the 10 membered-ring (MR) channel) were calculated by geometry optimization, this time allowing the TMA molecules to relax. A net molecular TMA charge of +1 was used in this calculation (the atomic charge distribution was obtained by the charge-equilibration method, setting the total charge to +1), which was compensated by the framework by using a modified version of the uniform charge background method,[17] where the atomic charge for every silicon atom was reduced until charge neutrality was achieved (i.e., to 2.3722).

This first set of calculations showed the preferential location of TMA molecules within the FER cavities; therefore, bmp molecules were required to be inserted in the 10 MR channels. Two different packing values for the bmp molecules have been studied, 2 or 1.33 bmp molecules per unit cell. In addition, two packing approaches were tried, with benzyl rings on opposite sides or on the same side. Thus, a zeolite model composed of 6 unit cells along the 10 MR channel axis (*c*-direction: 1 × 1 × 6 supercell) was used, where 12 (6 on each 10 MR channel, 2 per unit cell) or 8 (4 on each 10 MR channel, 1.33 per unit cell) bmp molecules were loaded in the required orientations. In addition, TMA molecules were located in every cavity (2 TMAs per unit cell). Atomic charges for the organic molecules were again calculated by the charge-equilibration method, setting the total net charge to +1 for each organic molecule (TMA or bmp). This net molecular charge was compensated by the framework in the same way as before, reducing the atomic charge for every silicon atom until charge neutrality. In this way, the silicon atomic charge was reduced to 2.2889 or to 2.3074 for the 2 and 1.33 bmp packing values, respectively. The oxygen atomic charge was fixed to −1.2.

Final location and interaction energies of the SDA molecules were obtained by a simulated annealing procedure.[18] This used constant NVT ensembles and time-steps of 1.0 fs. The simulated annealing procedure consisted first of heating from 300 K with temperature increments of 10 K until 700 K and then cooling in the same way until 300 K; 500 steps (0.5 ps) were run in every heating and cooling step. This protocol was repeated 10 times, and the most stable situation was taken. The final interaction energies were calculated by subtracting the energy of the isolated molecules optimized in vacuo from the total energy of the system. All the interaction energies are expressed in kcalories per mole.

Results

Hereafter, the samples will be named making reference to the SDAs used in their synthesis. The samples synthesized in the presence of two SDAs will be referred to with the names of these two cations. The samples with bmp and TMA will be named bmp-TMA-1, for samples with TMA/Al = 1, and bmp-TMA-2 for samples with TMA/Al = 0.2. The experiments are summarized in Table 1.

It has been reported elsewhere[19] that the use of bmp alone as a SDA leads to a mixture of at least three yet unidentified phases, according to SAED-TEM results. On the contrary, XRD patterns of the bmp-TMA-1 preparations at selected heating times (Figure 1) indicate that ferrierite was obtained as a pure phase, as was further confirmed by TEM studies (not shown).

Ferrierite is a medium-pore zeolite whose structure (natural single crystal) was first determined in the orthorhombic space group *Immm*.[20] The space group has been the subject of some discussion, and a reduction of symmetry to *Pmnn* has been reported.[21−23] The FER framework is based on chains of

(14) Dauger-Osguthorpe, P.; Roberts, V. A.; Osguthorpe, D. J.; Wolff, J.; Genest, M.; Hagler, A. T. *Proteins: Struct., Funct., Genet.* **1988**, *4*, 21.
(15) *Sorption Module*, version 4.6; Accelrys Inc.: San Diego, 2001.
(16) Rappe, A. K.; Goddard W. A., III. *J. Phys. Chem.* **1995**, *95*, 3358.
(17) De Vita, A.; Gillan, M. J.; Lin, J. S.; Payne, M. C.; Stich, I.; Clarke, J. L. *Phys. Rev. B* **1992**, *46*, 12964.
(18) *Dynamics Simulation*, version 4.6; Accelrys Inc.: San Diego, 2001.
(19) Pinar, A. B.; Garcia, R.; Arranz, M.; Perez-Pariente, J. Co-directing role of template mixtures in zeolite synthesis. 15th International Zeolite Conference, Beijing, 2007; Vol. 1, p 383.
(20) Vaughan, P. A. *Acta Crystallogr.* **1966**, *21*, 983.
(21) Meier, R.; Ha, T. K. *Phys. Chem. Miner.* **1980**, *6*, 37.
(22) Morris, R. E.; Weigel, S. J.; Henson, N. J.; Bull, L. M.; Janicke, M. T.; Chmelka, B. F.; Cheetham, A. K. *J. Am. Chem. Soc.* **1994**, *116*, 11849.
(23) Weigel, S. J.; Gabriel, J. C.; Gutierrez-Puebla, E.; Monge-Bravo, A.; Henson, N. J.; Bull, L. M.; Cheetham, A. K. *J. Am. Chem. Soc.* **1996**, *118*, 2427.

Table 1. Gel Compositions and Products Obtained[a]

gel	SDAs	*t* (days)	Si/Al gel	TMA/Al gel	TMA/T[b] gel	pH gel	product
bmp	Bmp	10					amorphous
		45	15.7				MP[c]
		98					MP[c]
bmp-TMA-1	TMA + bmp	10					FER[d]
		20	15.7	1	0.06	10.2	FER[d]
		30					FER[d]
		83					FER[d]
bmp-TMA-2	TMA + bmp	10					FER[d]
		20	15.7	0.2	0.012	8.9	FER[d]
		143					FER[d]
TBA−TMA	TMA + TBA	6	15.7	1	0.06	10.3	amorphous
		11					amorphous
TMA	TMA	7					U[e]
		10	15.7	9	0.54	9.3	U[e]
		20					U[e]
bmp-TMA-3	TMA + bmp	7	11	0.75	0.06	9.8	FER[d]
		10					FER[d]
bmp-TMA-4	TMA + bmp	10	35	2.1	0.06	9.5	AST
		20					AST

[a] Gel composition for bmp-TMA samples is x TMAOH/(0.54 − x) bmpOH/0.48 HF/0.031 Al_2O_3/0.969 SiO_2/4.6 H_2O, where x is 0.06 (bmp-TMA-1) or 0.012 (bmp-TMA-2). For the TBA−TMA samples, the gel composition is the same as in bmp-TMA-1 but with TBA instead of bmp. In syntheses with only one SDA, the total concentration of organic compounds is the same, that is, 0.54 bmp (bmp samples) or 0.54 TMA (TMA samples). [b] Ratio of TMA to total amount of Si + Al present in the synthesis gel. [c] Mixture of phases. [d] Ferrierite. [e] Unidentified crystalline product.

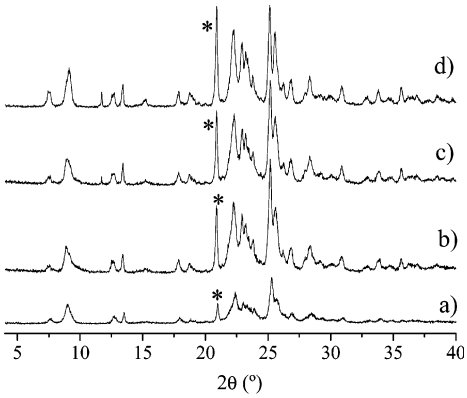

Figure 1. XRD patterns of samples obtained from bmp-TMA1 gel after 10 (a), 20 (b), 30 (c), and 83 (d) days of heating at 150 °C. The peak highlighted with an asterisk probably corresponds to a dense phase.

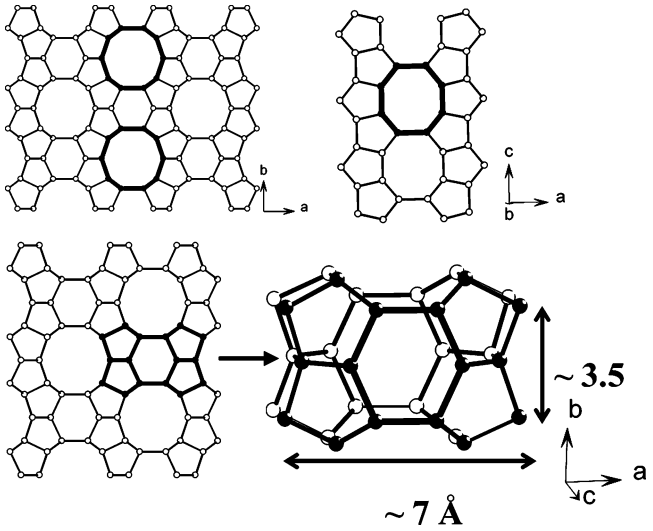

Figure 2. Ferrierite structure: 10 MR channel view along the *c*-axis (up, left) and 8 MR channel view along the *b*-axis (up, right) and FER cavity view along the *c*-axis (down).

5-membered rings (5 MR), which are linked to give [5^4] polyhedral units. There are two types of perpendicularly intersecting channels in the structure. The main channel is parallel to the orthorhombic *c*-axis of the crystal and is outlined by elliptical 10 MR (4.3 Å × 5.5 Å diameter), while the side channel, along the *b*-axis, is formed by 8 MR (3.4 Å × 4.8 Å in diameter). There are also 6-membered rings that form a channel parallel to the *c*-axis. The intersection of this channel with the 8 MR channel forms an elliptical cavity called the FER cavity[24] or [$5^8 6^6 8^2$] (see Figure 2). The inner dimensions of this cavity are about 7 Å along the *a*-direction and approximately 3.5 Å in the *b*-direction. The unit cell of the ferrierite is constituted by 36 T atoms (atoms in tetrahedral coordination), and it contains two FER cavities.

XRD patterns of samples obtained at different heating times ranging from 10 to 83 days show that, under these synthesis conditions, ferrierite is a stable phase, whose crystallinity increases with heating time. This results in evidence of the fundamental role of TMA in crystallizing this pure FER phase instead of the mixture of phases obtained in its absence. In fact, TMA was the first quaternary ammonium cation used for the synthesis of ferrierite,[25] although in that case, Na^+ was also present in the synthesis gel. Since then, many N-containing compounds as well as oxygenated hydrocarbons (THF[26] and 2,4-pentane-2,4-dione[27]) have been used in its synthesis. Among N-containing compounds, aliphatic amines have been widely employed as SDAs of ferrierite, for instance, diethanolamine,[28] 1,3-diaminopropane,[29] and ethylenediamine,[30] in alkaline aqueous media in the presence of inorganic cations (usually Na^+). Cyclic amines, such as pyrrolidine[31,32] and piperidine,[33]

(24) http://www.iza-structure.org/databases.

(25) Kibby, C. L.; Perrotta, A. J.; Massoth, F. E. *J. Catal.* **1974**, *35*, 256.
(26) Guo, G. Q.; Sun, Y. J.; Long, Y. C. *Chem. Commun.* **2000**, *19*, 1893.
(27) Kaduk, J. A. Synthesis of molecular sieves using beta-diketones as organic templates. U.S. Patent 4,323,481, 1982.
(28) Forbes, N.; Rees, L. V. C. *Zeolites* **1995**, *15*, 444.
(29) Valyocsik, E. W.; Rollmann, L. D. *Zeolites* **1985**, *5*, 123.
(30) Jacobs, P. A.; Martens, J. A. *Stud. Surf. Sci. Catal.* **1987**, *33*, 8.
(31) Jongkind, H.; Datema, K. P.; Nabuurs, S.; Seive, A.; Stork, W. H. J. *Microporous Mater.* **1997**, *10*, 149.
(32) Xu, W. Q.; Yin, Y. G.; Suib, S. L.; Edwards, J. C.; O'Young, C. L. *J. Phys. Chem.* **1995**, *99*, 9443.

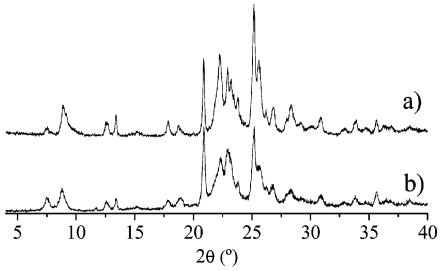

Figure 3. XRD patterns of samples obtained from (a) bmp-TMA-1 and (b) bmp-TMA-2 gels after 20 days of hydrothermal treatment.

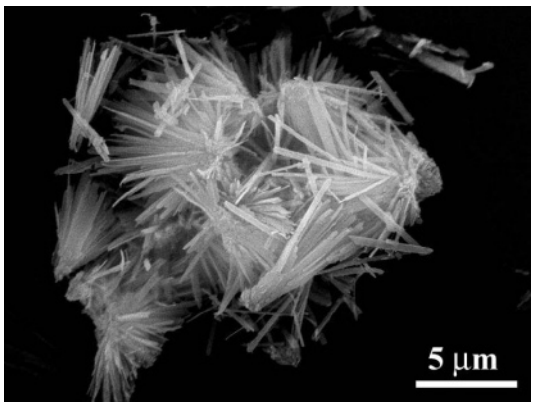

Figure 4. SEM image of sample obtained from bmp-TMA-1 gel after 30 days of hydrothermal treatment.

have also been employed, both in alkaline and in fluoride media.

To further investigate the role of TMA in the crystallization process of the FER structure, we drastically reduced the amount of TMA in the gel (gel bmp-TMA-2). In these experiments, the amount of TMA is 5 times lower than that in the bmp-TMA-1 gel, giving a TMA/Al ratio in the gel of 0.2. The XRD patterns show that ferrierite is also obtained under these synthesis conditions, although the peaks are slightly less defined (see Figure 3). We carried out an experiment at longer crystallization times to assess the stability of ferrierite. After 143 days of hydrothermal treatment of bmp-TMA-2 gel, ferrierite is still the product obtained, according to the XRD pattern, thus showing that, under these synthesis conditions, ferrierite is also a stable phase.

Once it was demonstrated that even with a low TMA content in the synthesis gel, ferrierite is obtained, we studied more in detail one sample obtained from the gel where TMA/Al = 1 (bmp-TMA-1 gel). SEM images of the sample obtained after 30 days of heating (Figure 4) show that it is constituted by elongated needles, the length of which is of the order of 10 μm.

The Si/Al ratio, as measured by chemical analysis (ICP-AES), was found to be 15.6, without substantial differences with the heating time, which is very close to the Si/Al ratio of the synthesis gel (15.7). Assuming that all the aluminum is incorporated in the zeolite lattice, as will be demonstrated by ^{27}Al NMR, this value is equivalent to 2.2 Al/unit cell.

The TGA analysis of the sample obtained after 20 days of heating is shown in Figure 5(line a). Three weight losses

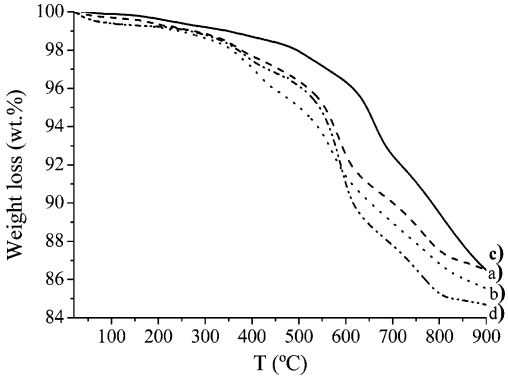

Figure 5. Thermogravimetric analysis of samples obtained from bmp-TMA-1 (a) and bmp-TMA-2 (b) gels after 20 days of heating, sample obtained from TMA gel after 10 days (c), and sample obtained from bmp-TMA-3 gel after 7 days (d).

Table 2. CHN and Organic Content of Products Obtained

		chemical analysis (wt %)				TGA	
gel	*t* (days)	C	H	N	C/N	organic (wt %)	product
bmp	10						amorphous
	45						MP[a]
	98						MP[a]
bmp-TMA-1	10	8.85	1.84	1.68	6.1	13.5	FER[b]
	20	9.30	1.83	1.73	6.3	13.7	FER[b]
	30	8.79	1.79	1.65	6.2	12.9	FER[b]
	83	8.40	1.66	1.62	6.0	11.7	FER[b]
bmp-TMA-2	10	10.97	2.07	1.67	7.7	16.5	FER[b]
	20	9.92	1.82	1.61	7.2	14.1	FER[b]
	143	9.19	1.81	1.61	6.7	11.6	FER[b]
TBA−TMA	6						amorphous
	11					11.3	amorphous
TMA	7	6.63	2.34	2.13	3.6	11.9	U[c]
	10	7.90	2.34	2.43	3.8		U[c]
	20	5.44	2.24	1.91	3.3		U[c]
bmp-TMA-3	7	9.55	2.11	1.91	5.8	14.3	FER[b]
	10	9.64	2.11	1.99	5.7		FER[b]
bmp-TMA-4	20	4.75	1.96	1.39	5.0	9.8	AST
	30	4.81	1.96	1.28	4.4		AST

[a] Mixture of phases. [b] Ferrierite. [c] Unidentified crystalline product.

were found, at around 370, 760, and the most intense one at ca. 560 °C. The samples are remarkably water-free (TG loss <0.5 wt % at T < 150 °C), as has been reported for many other high-silica zeolites synthesized in the presence of a F^- anion. According to TGA results, the organic content of all the samples obtained from the bmp-TMA-1 gel was around 13 wt %, similar to the amount of organic occluded commonly reported for ferrierite.[34,35]

According to the chemical analysis results, the nitrogen content of the samples was approximately 0.12 molar %, which is equivalent to 3 N atoms per unit cell. The C/N ratio, as measured by chemical analysis, was about 6.3 (Table 2). This ratio is between those of the two molecules employed as SDAs, bmp (C/N =12) and TMA (C/N =4), thus suggesting that both cations are incorporated within the zeolitic structure, probably incorporating more TMA than bmp. However, this analysis was not able to confirm the integrity of bmp molecules within the FER structure; it had to be demonstrated by means of ^{13}C NMR.

(33) Nanne, J. M.; Post, M. F. M.; Stork, W. H. J. Process for the preparation of ferrierite. EP Patent 12,473, 1980.

(34) Weigel, S. J.; Gabriel, J. C.; Gutierrez-Puebla, E.; Monge-Bravo, A.; Henson, N. J.; Bull, L. M.; Cheetham, A. K. *J. Am. Chem. Soc.* **1996**, *118*, 2427.

(35) Pál-Borbély, G.; Beber, H. K.; Kiyozumi, Y.; Mizukami, F. *Microporous Mesoporous Mater.* **1998**, *22*, 57.

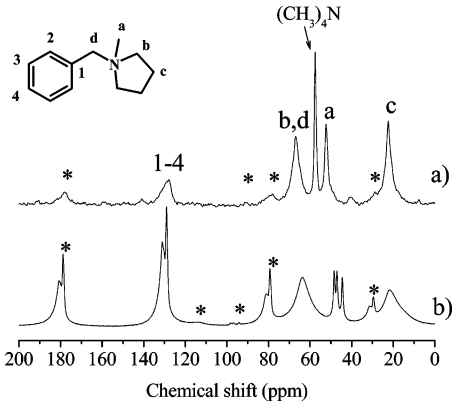

Figure 6. ^{13}C CP/MAS NMR spectra of (a) sample obtained from gel bmp-TMA-1 after 30 days of heating and (b) bmp cation as its iodide salt (asterisk: spinning side bands).

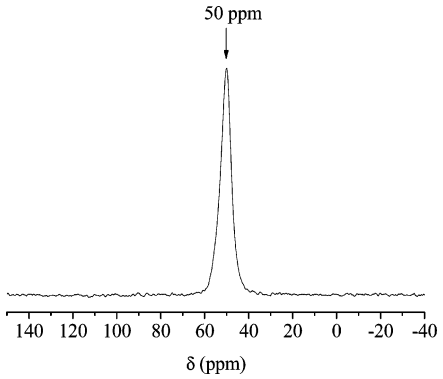

Figure 7. ^{27}Al NMR spectrum of sample obtained from bmp-TMA-1 gel after 30 days of heating at 150 °C.

In Figure 6, the ^{13}C NMR spectrum of the sample obtained after 30 days of hydrothermal treatment is shown together with the spectrum of bmp iodide salt for comparison. The signal at 23 ppm is assigned to the CH_2 groups in the β position in the pyrrolidine ring; the signal at 67 ppm corresponds to both the CH_2 groups linked to the nitrogen atom in the pyrrolidine ring and the methylene group bringing the aromatic and pyrrolidine rings. The resonance at 53 ppm is assigned to the CH_3 group linked to the nitrogen atom, and finally, the signal at 129 ppm corresponds to the carbon atoms of the aromatic ring. Therefore, all the signals corresponding to the bmp cation are observed, which confirms the resistance of this cation to the hydrothermal process and its integrity inside the ferrierite structure. The spectrum displays an additional signal at 57.4 ppm, which cannot be assigned to the bmp molecule, but appears in the typical range of the TMA cations trapped in zeolitic cages;[36,37] therefore, it was assigned to the presence of this cation occluded within the ferrierite structure.

The incorporation of aluminum either in framework or in out-of-lattice (extra-framework) positions was investigated by ^{27}Al MAS NMR spectroscopy. The ^{27}Al NMR spectrum of the sample obtained from the bmp-TMA-1 gel after 30 days of heating is shown in Figure 7 and consists of one sharp single line at 50 ppm attributed to tetrahedral aluminum in the zeolite lattice. The absence of any signal at around 0 ppm indicates that there is no aluminum in octahedral coordination, which suggests that all the aluminum is incorporated in the zeolite lattice.

As mentioned previously, the samples show a nitrogen content of 3 N atoms per unit cell of ferrierite, which is higher than the aluminum content (about 0.07 molar %, 2.2 Al per unit cell). Therefore, not all the positive charges of the cations employed as SDAs are compensated by the negative charges generated by the isomorphous substitution of Si by Al in the lattice. The excess of positive charges could be counterbalanced by connectivity defects, but in this case, as the synthesis has been carried out in fluoride medium, the inclusion of the F^- anion in the final zeolite would be a more likely mechanism for charge balance. Indeed, ^{19}F MAS NMR shows the presence of a signal of fluorine atoms at −77.0 ppm (not shown). Besides, the spectrum displays a low signal-to-noise ratio, which suggests that the amount of fluoride occluded within the FER structure is low. This is in agreement with the fact that more than 70% of the positive charges is counterbalanced by the Al present in the zeolite lattice. ^{19}F MAS NMR has been shown to be very useful to obtain information on the location of fluoride anions within zeolite cavities,[38] as in some cases it has been found that there is a relationship between the chemical shift of the signal and the type of cage occupied by F^-. In particular, in the case of ferrierite, several XRD studies have found the F^- anion occluded in the [5^4] cage.[39,40] The NMR signal of fluoride inside these cages has been reported to appear between −59.5 and −56.4 ppm;[41] therefore, the chemical shift of −77.0 ppm suggests in this case a different location for the F^- anions retained in the structure.

Once it was demonstrated that both cations employed as SDAs keep their integrity within the ferrierite structure, it was interesting to investigate the effect of the variation of the Si/Al ratio in the synthesis gel. In these experiments, the composition of the SDAs has been fixed to be the same as in the bmp-TMA-1 experiment. In that case, the Si/Al ratio in the gel was 15.7, which implies that there were ∼2 Al atoms per unit cell, while the nitrogen content of ca. 3 nitrogen atoms per unit cell indicated the presence of 3 cations (TMA or bmp) in each unit cell of ferrierite. Therefore, in principle, it could be thought that this zeolitic structure could accommodate in the lattice a maximum of 3 Al atoms per unit cell, as the negative charges would be counterbalanced by the positive ones. In an attempt to demonstrate this fact, we performed a synthesis decreasing the Si/Al ratio in the gel to 11 (bmp-TMA-3 gel). In these conditions, and assuming a quantitative yield of T atoms, the resulting ferrierite would contain 3 Al/unit cell. The XRD patterns of the products obtained (see Figure 8) correspond

(36) Fan, W.; Shirato, S.; Gao, F.; Ogura, M.; Okubo, T. *Microporous Mesoporous Mater.* **2006**, *89*, 227.
(37) Hayashi, S.; Suzuki, K.; Hayamizu, K. *J. Chem. Soc., Faraday Trans. 1* **1989**, *85*, 2973.
(38) Delmotte, M.; Soulard, M.; Guth, F.; Seive, A.; López, A.; Guth, J. L. *Zeolites* **1990**, *10*, 778.
(39) Villaescusa, L. A.; Bull, I.; Wheatley, P. S.; Lightfood, P.; Morris, R. E. *J. Mater. Chem.* **2003**, *13*, 1978.
(40) Attfield, M. P.; Weigel, S. J.; Taulelle, F.; Cheetham, A. K. *J. Mater. Chem.* **2000**, *10*, 2109.
(41) Villaescusa, L. A.; Camblor, M. A. *Recent Res. Dev. Chem. Sci.* **2003**, *1*, 93.

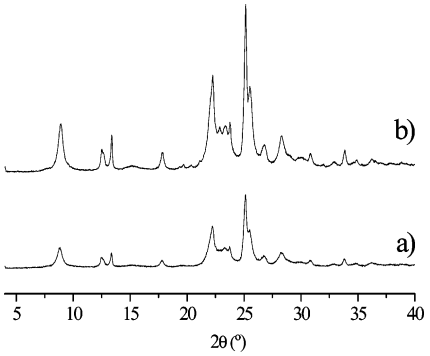

Figure 8. XRD patterns of samples obtained from bmp-TMA-3 gel after 7 days (a) and 10 days (b) of hydrothermal treatment.

indeed to ferrierite, although the samples show an apparent lower crystallinity than the solids obtained from Al-poor gels.

The organic content of these samples is higher than the amount of organic occluded in the solids obtained from Al-poor gels (see Figure 5). Both samples show a similar weight loss at low temperatures ($T < 550$ °C), while at higher temperatures, the samples with a Si/Al ratio in the gel of 11 have a higher weight loss (10 wt %). Moreover, it is interesting to notice that the C/N ratio of the solid products decreases as the Al in the lattice increases, thus suggesting that TMA is preferred over bmp for charge compensation.

Furthermore, we performed a synthesis increasing the Si/Al ratio in the gel to 35 (samples bmp-TMA-4), corresponding to 1 Al atom per unit cell of ferrierite. However, in this case, the XRD pattern of the solid obtained corresponds to octadecasil (AST). This clathrasil is formed by [$4^6 6^{12}$] cages connected by [4^6] hexahedral cages (double four rings). Caullet et al. and Xang[42] have reported the synthesis of this material in fluoride medium, employing a TMA cation as SDA. They were able to locate the TMA cation accommodated in the [$4^6 6^{12}$] cages, while the F^- anion occupied the smaller [4^6] cages. The unit cell composition was found to be $|[N(CH_3)_4^+]_{2.0}F^-_{1.9}|[Si_{20}O_{40}]$. The octadecasil framework contains two [$4^6 6^{12}$] cages and two [4^6] cages per unit cell; therefore, there is one TMA cation in each [$4^6 6^{12}$] cage. In our case, the nitrogen content calculated from the TGA analysis assuming that all the organic weight loss is due to TMA resulted in 1.7 N atoms per unit cell of octadecasil. Therefore, although it is an approximated estimation, it is close to the reported two TMA cations per unit cell of AST. The C/N ratio of these materials is about 4.4, thus demonstrating that only the TMA cation is incorporated to the framework, as the bmp cation is too large to be accommodated within the AST structure.

Computational Results: SDA Location. There are two possible locations for the SDA molecules in this structure: they can be occluded either in the cavity or in the 10 MR channel. The bmp molecules are too large to be accommodated in the FER cavities, so they will be located in the larger 10 MR channels. However, TMA cations can be occluded in both types of locations.

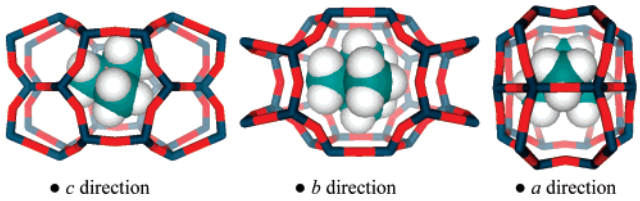

Figure 9. Three views of the TMA molecules occluded within the FER cavity.

(i) Insertion of TMA Molecules. First of all, we studied the most stable location for the TMA molecules by using Monte Carlo simulations. Both simulation pressures (100 or 1000 kPa) resulted in an insertion of two TMA molecules per unit cell, each one located in the center of the FER cavities. This results in evidence of the great preference of TMA molecules for being located in such cavities, due to the perfect adjustment between the spherical shape of the TMA molecule and the FER cavity (Figure 9). Nevertheless, there exists another possible location for the TMA molecules, which is within the 10 MR channel. We calculated the interaction energy of the TMA molecule for both locations by geometry optimization, resulting in −101.6 and −92.1 kcal/mol per molecule for TMA trapped in the cavities or located in the 10 MR channel, respectively. This result again demonstrates the clear preferential location of TMA filling the FER cavities.

(ii) Insertion of bmp Molecules. Once the location of the TMA molecules within the cavities was demonstrated, we studied the incorporation of the bmp molecules. As previously explained, these molecules are too large to be accommodated inside the cavities, so their only possible location is inside the 10 MR channel. The occlusion of TMA molecules in the cavities makes possible a treatment of the system as a one-dimensional system since the connection between different 10 MR channels is through such filled cavities. First of all, we studied the possibility of forming supramolecular assemblies (dimers) through overlapping of the aromatic rings parallel to each other, similar to those we have previously observed[43,44] in AlPO materials synthesized with other organic molecules containing an aromatic ring. In this case, these dimers were broken after geometry optimization due to the small size of the 10 MR channels, which does not allow the location of benzyl rings parallel to each other; this results in evidence that these bmp molecules will not assemble as dimers inside the FER structure.

When looking at the bmp molecular dimensions, we realized that two possible packing values are possible to fit in a commensurate way in the ferrierite unit cell: 2 molecules per 1.5 unit cells (1.33 each unit cell) or 2 per each unit cell (one on each 10 MR channel). Besides, two bmp approachings are possible, with benzyl rings in opposite sides (referred as opposite) or in the same side, facing each other (although without overlapping benzyl rings, as previously explained) (referred to as faced). The interaction energies for all the possibilities were calculated by the simulated annealing

(42) (a) Caullet, P.; Guth, J. L.; Hazm, J.; Lamblin, J. M.; Gies, H. *Eur. J. Solid State Inorg. Chem.* **1991**, *28*, 345. (b) Yang, X. *Mater. Res. Bull.* **2006**, *41*, 54.

(43) Gomez-Hortiguela, L.; Cora, F.; Catlow, C. R. A.; Perez-Pariente, J. *J. Am. Chem. Soc.* **2004**, *126*, 12097.

(44) Gomez-Hortiguela, L.; Perez-Pariente, J.; Cora, F.; Catlow, C. R. A.; Blasco, T. *J. Phys. Chem. B* **2005**, *109*, 21539.

Table 3. Interaction Energies[a] for Different Packing and Approaches

model		organic (per unit cell)		total energy	vdW	Coulomb
packing	approach	TMA	bmp	(per unit cell)	energy	energy
1.33	Opposite	2	1.33	−416.28	−70.69	−351.65
	Faced	2	1.33	−422.34	−76.32	−350.35
2	Opposite	2	2	−298.62	+60.95	−436.44
	Faced	2	2	−241.73	+123.24	−435.22

[a] Expressed in kcal/mol per unit cell.

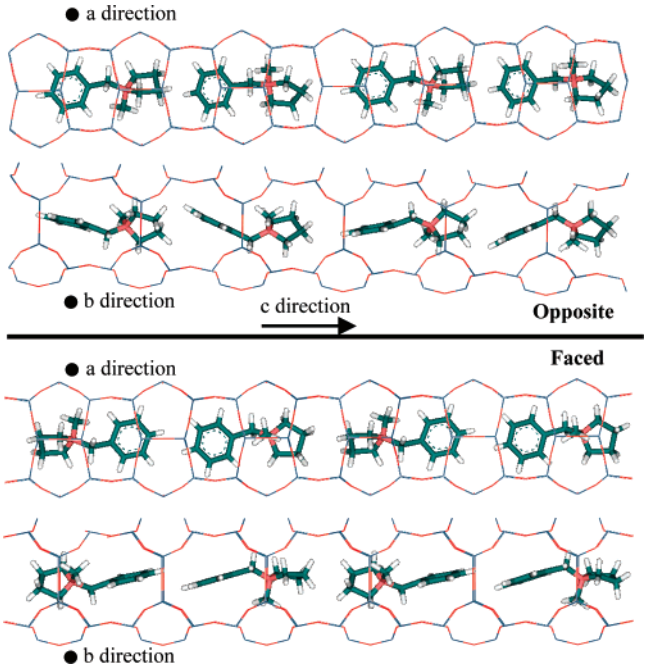

Figure 10. Two views of the final location of bmp molecules in the 8/6 packing model (1.33 molecules per unit cell) in the opposite (top) or faced (bottom) approach.

procedure, employing a 1 × 1 × 6 unit cell FER system and loading the TMA molecules in the cavities (2 per unit cell) and the corresponding bmp molecules (12 or 8 per 6 unit cell) in the required orientations. Energy results are shown in Table 3.

First, we can clearly observe that the packing of 2 bmp molecules per unit cell is unstable in either the opposite or the faced approaches. This indicates that the FER structure is not able to accommodate such a high number of molecules since they must be very constrained inside the microporous structure. However, the interaction energy for the packing value of 1.33 molecules per unit cell is extremely high in both approachings (more negative), which demonstrates that bmp molecules fit much better within the FER structure under this packing value. Figure 10 shows the location of bmp molecules along the 10 MR channel in both approaches. In both cases, the aromatic rings are located nearly parallel to the *b*-direction (perpendicular to the *a*-direction); this is due to the elliptical nature of the 10 MR channel, which is longer in the *b*-direction than in the *a*-direction and thus allows a better fitting if the aromatic ring is located parallel to the b-direction. It can also be noticed that the most stable approach is when the benzyl rings are facing each other, which suggests that there exists a stabilizing interaction between adjacent aromatic rings, although they do not form dimers.

Discussion

From the previous results, the TMA cation has proven to play a key role in the crystallization of the ferrierite structure, as this zeolite does not crystallize when bmp is employed as the only SDA. The incorporation of TMA to the zeolite framework has been confirmed by ^{13}C MAS NMR, which has demonstrated itself to be a useful technique to identify the local environment of organic cations occluded in zeolite structures. Concerning TMA trapped in various zeolite pores and cages, Hayashi et al.[11,37] were able to correlate the observed chemical shift with the diameter of the zeolite cage in which the TMA species are occluded, measured as the size of the largest sphere that can be drawn within the cage. In that work, the ^{13}C CP/MAS NMR spectra of several zeolites synthesized in the presence of TMA were recorded. All the zeolites contained one or more cages that were able to accommodate TMA cations, for example, the sodalite and α cavities, in zeolite LTA, or the gmelinite cavity, in zeolites gmelinite and offretite. These authors found that the signal assigned to the methyl groups of the TMA cations appears at higher chemical shifts as the size of the cage trapping this cation decreases. According to these correlations, in our case, TMA cations would be trapped in a cage having a size between 7.6 and 8.7 Å, making the ferrierite cavity the most likely location of this cation and discarding the 10 MR channel (cross-section = ∼5.0 Å) as the TMA host. Moreover, the existence of only one symmetric signal assigned to the methyl groups of the TMA of the sample obtained from the bmp-TMA-1 gel after 30 days of heating (Figure 6) suggests that all the TMA cations occluded within the ferrierite framework are located in a similar chemical environment, the FER cages, in agreement with the computational study.

As has been already mentioned, samples obtained from the bmp-TMA-1 gel contain about 3 N atoms per unit cell. The calculated packing value from the computational results was 2 TMA cations and 1.3 bmp cations per unit cell of ferrierite, making a total of 3.3 nitrogen atoms per unit cell, in good agreement with the experimental results. Besides, the amount of TMA per unit cell in the gel was 2.1, very close to the amount of TMA in the final zeolite product suggested by the computational results. Therefore, as the yield in oxide is high (about 90%), it suggests that every FER cage is occupied by one TMA cation. This selectivity of zeolite cages toward TMA cations was already observed by Aiello et al. In 1970, Aiello and Barrer[8] synthesized several zeolites employing TMA combined with an inorganic cation (Na^+ or K^+) as SDAs. All these zeolites contained cages in their frameworks, for example, sodalite, which contains sodalite cages, omega and offretite, which contain the gmelinite cage, and erionite, the erionite cage. These authors observed a strong tendency of TMA cations to be accommodated within these cages and to avoid almost completely the wide channels.

In the experiment bmp-TMA-2, we studied the system behavior when the amount of TMA in the gel was not sufficient to fill all the FER cavities. In this case, there were only 0.4 (instead of 2) TMA cations per unit cell in the gel. In these conditions, the only possibility for TMA to fill the

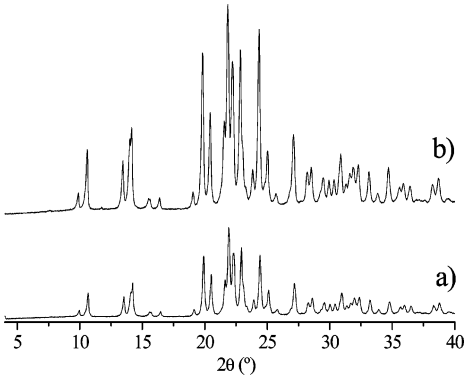

Figure 11. XRD patterns of samples obtained from TMA gels after (a) 7 days and (b) 10 days of hydrothermal treatment.

two cavities of ferrierite per unit cell would be that the nucleation and growth of the crystals finished when there was no more TMA available in the gel. Such a crystallization process would lead to a large amount of amorphous material accompanying the FER crystals; however, the crystallinity of the resulting material is relatively high. Therefore, a small amount of TMA in the gel was able to promote the crystallization of ferrierite, which proceeds although the synthesis gel is depleted of TMA. This observation suggests that the TMA cation has a nucleating role in the crystallization of ferrierite.

In an attempt to further understand the role of each one of the two cations employed as SDAs, TMA and bmp, we carried out syntheses in the presence of only one of them. The compositions of the gels in all the experiments have been set to maintain a constant total concentration of organic species, as was specified in the Experimental Procedures. As was already mentioned, in the samples obtained from the bmp gel (see Table 1), synthesized with the bmp cation as the only SDA, a mixture of at least three different phases was obtained. Therefore, the presence of a cation that fits in the cavities of the ferrierite seems to be required to obtain this zeolite.

Now, the question arises as to whether the crystallization of this framework requires the presence of a bmp cation. In an attempt to answer this question, we carried out a subsequent experiment (TBA−TMA gel, Table 1) in which we replaced the bmp cation by TBA, which, due to its size, is not able to be accommodated within the ferrierite structure. The resulting product was an amorphous material. Hence, we can conclude that the bmp cation plays a specific role in the crystallization of ferrierite. Moreover, if only TMA is present in the synthesis gel at high concentrations, a crystalline product whose XRD pattern (Figure 11) does not correspond to ferrierite is obtained. The XRD patterns of the products obtained at different heating times are similar, and we do not observe substantial variations in the relative intensities of the peaks that would suggest the presence of more than one crystalline phase. Therefore, it seems that this as yet unidentified product is likely a pure phase, and it is currently being studied in our lab for structure identification.

All these results demonstrate that both types of molecules are required to be present in the synthesis medium to allow the crystallization of this structure: in the absence of the TMA cation, a mixture of phases is obtained, while the absence of bmp yields either a crystalline product different from ferrierite or, if it is substituted by TBA, an amorphous material. On the basis of these observations, we conclude that both SDAs play a co-structure directing effect during the crystallization of the FER structure, in what becomes a new example of a cooperative structure directing effect in the synthesis of microporous materials.[45] Aiello and Barrer, in one of the earliest publications in which the templating concept was first used, already suggested that the affinity observed between TMA cations and several zeolitic cavities may play an important part in their synthesis, through a template action involving the association of TMA and the aluminosilicate precursors of the cavities. It is noteworthy that the ferrierite structure can be built-up just by linking the FER cavities, with no necessity of other building units to connect them. Therefore, we could think of the crystallization of the FER structure in this co-templated system as a condensation of the TMA-containing cages assisted by the presence of bmp cations, a process that is illustrated in Figure 12. However, from the results we have shown, it is not possible to determine whether the TMA-filled cavities preexist in the gel and they are subsequently assembled through the 10 MR or if, by contrast, the process cannot be separated in two steps and the formation of the cavities and their bmp-assisted assembling occurs simultaneously.

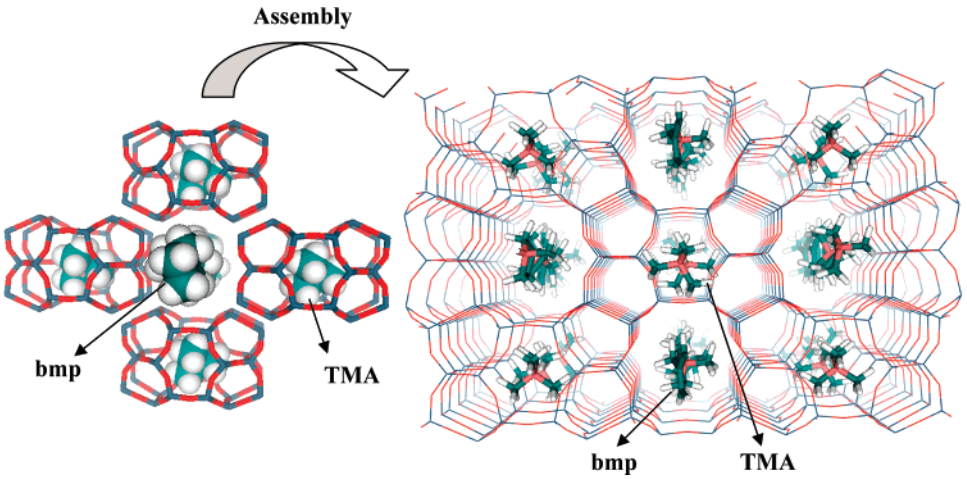

Figure 12. Scheme of the self-assembly of TMA-filled cavities around bmp molecules to give the final ferrierite structure.

To our knowledge, there is only one reference to the synthesis of ferrierite in fluoride media in the presence of a mixture of two SDAs. Kupperman et al. reported in their paper the synthesis of ferrierite with a mixture of pyridine and propylamine.[46] Nonetheless, both organic molecules are small enough to fit within the FER cavity, and hence, they do not show any preference to be accommodated either in the main 10 MR channel or in the cavity. Indeed, single-crystal XRD data have demonstrated that pyridine is located in the cavity as well as in the 10 MR channel, where it is accompanied by a small amount of propylamine, evidencing the lack of specificity of this mixture of SDAs.

Conclusion

In this work, we have rationally selected a combination of two SDAs to obtain open-framework zeolites. Following this synthesis strategy, the simultaneous use of TMA and the bulkier bmp as SDAs led to the crystallization of the zeolite ferrierite from gels having a Si/Al ratio in the range of 16−10, in fluoride medium and in the absence of inorganic cations. Both organic cations are found occluded inside the zeolite framework, and the ^{13}C NMR spectrum suggests that TMA is located inside the $[5^8 6^6 8^2]$ ferrierite cage. Molecular mechanics calculations revealed the templating role of both cations, as the most stable configuration of the system corresponds to the siting of TMA within the FER cages, while bmp accommodates in the 10-membered ring one-dimensional channels of the structure, being too large to be occluded inside the small cages. Indeed, both cations are required for the nucleation of this zeolite, furthermore evidence of their co-structure directing role in the crystallization process, for in the absence of either TMA or bmp, the synthesis gel fails in rendering ferrierite crystals.

Acknowledgment. A.B.P. acknowledges the Spanish Ministry of Education for a FPU grant. The authors gratefully acknowledge Dr. Teresa Blasco for recording the NMR spectra. This work has been financially supported by the CICYT (Project CTQ2006-06282).

CM071753O

(45) Arranz, M.; Perez-Pariente, J.; Wright, P. A.; Slawin, A. M. Z.; Blasco, T.; Gomez-Hortiguela, L.; Cora, F. *Chem. Mater.* **2005**, *17*, 4374.
(46) Kuperman, A.; Nadimi, S.; Oliver, S.; Ozin, G. A.; Garces, J. M.; Olken, M. M. *Nature (London, U.K.)* **1993**, *365*, 239.